

Fabrication of SiC microelectromechanical systems using one-step dry etching

Liudi Jiang^{a)} and R. Cheung

School of Engineering and Electronics, Scottish Microelectronics Centre, The University of Edinburgh, King's Buildings, West Mains Road, Edinburgh EH9 3JF, United Kingdom

M. Hassan and A. J. Harris

School of Electrical, Electronics and Computer Engineering, University of Newcastle Upon Tyne, Newcastle NE1 7RU, United Kingdom

J. S. Burdess

School of Mechanical and Systems Engineering, University of Newcastle Upon Tyne, Newcastle NE1 7RU, United Kingdom

C. A. Zorman and M. Mehregany

Department of Electrical Engineering and Computer Science, Case Western Reserve University, Cleveland, Ohio 44106

(Received 1 July 2003; accepted 29 September 2003; published 10 December 2003)

A simple one-step inductively coupled plasma etching technique has been developed for the fabrication of SiC resonant beam structures. Straight cantilever and bridge devices have been made successfully. The structures have been actuated and resonant frequencies ranging from ~ 120 kHz to ~ 5 MHz have been measured. Comparison of the theoretically simulated and experimentally measured resonant frequencies shows the presence of significant tensile stress in bridge structures while the cantilever beams are free of stress. The degree of the tension in the bridge structures has been found to be independent of the bridge length. © 2003 American Vacuum Society.

[DOI: 10.1116/1.1627804]

I. INTRODUCTION

Although micromachining techniques for silicon (Si) are well developed and a range of silicon microelectromechanical systems (MEMS) have been fabricated, Si MEMS are not suitable for use in harsh environments including locations of high temperature, high frequency, high wear, and corrosive media. In contrast, silicon carbide (SiC) is an excellent candidate for microsensors and microactuators for use in extreme conditions due to its outstanding physical and chemical properties.¹ In particular, because of the high Young's modulus (E) of SiC and the relatively low-mass density (ρ), the larger ratio of $\sqrt{E/\rho}$ will result in significantly higher resonant frequencies for SiC beam structures compared to their silicon and gallium arsenide counterparts.²

Micromachined SiC resonant devices have been fabricated in the past, these include pressure sensors,¹ lateral resonant structures,³ and micromotors.⁴ However, most of the fabricated devices make use of bulk micromachining or micromolding techniques that tend to be more complex than surface micromachining. Significant bending effect has also been observed in released cantilever beams, especially in longer beam structures. The bending effect has been attributed to the result of a bending moment induced by a residual stress gradient through the film thickness¹ and also due to surface tension encountered in the wet etch processes. In addition, comparing with dry etching techniques, there is also less control of etch rates and etch profiles using wet etch to release resonance structures.

Recently, nanoelectromechanical systems have been fabricated using surface micromachining techniques and a two-step dry-etch process.² In this paper, we report on a simple one-step dry-etch process for the fabrication of released SiC cantilevers and bridges. This simplified dry-etch method avoids the potential damage due to surface tension and the lack of control on etch rates and etch profiles encountered in wet etch processes. The fabricated cantilever and bridge structures have been successfully actuated and the fundamental resonant frequencies have been measured and compared theoretically with simulated data.

II. FABRICATION AND TESTING

The starting material is nominally undoped $2\ \mu\text{m}$ thick single-crystalline 3C-SiC film heteroepitaxially grown on Si (100) wafers. The details of the 3C-SiC growth using a two-step, carbonization-based, atmospheric pressure chemical vapor deposition process has been described elsewhere.⁵ After the samples had been ultrasonically cleaned in acetone and isopropanol, a $3\ \mu\text{m}$ thick SiO_2 etch mask layer has been deposited on the samples using plasma-enhanced chemical vapor deposition system. Photoresist (Megaposit SPR2-2FX 1.3) has been spun on top of the SiO_2 covered samples. Photolithography has been performed to pattern the oxide in the shape of the cantilevers and bridges. The cantilevers are of widths $15\ \mu\text{m}$ and of lengths 25, 50, 100, 150, 200 μm . The bridges have widths $15\ \mu\text{m}$ and lengths of 50, 100, 150, 200, 250 μm . After photoresist development, a plasmatherm

^{a)}Electronic mail: liudi.jiang@ee.ed.ac.uk

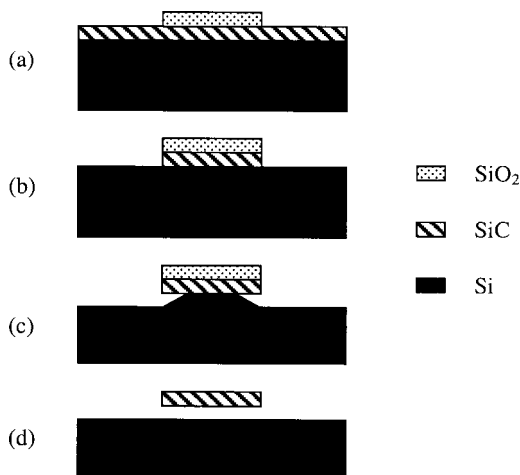


FIG. 1. (a)–(d) Schematic diagram of the processing steps to fabricate suspended SiC beams.

PK 2440 reactive ion etching system has been used to remove the patterned SiO₂ layer exposing the SiC underneath. The remaining photoresist has been removed using O₂ plasma. Subsequently, inductively coupled plasma (ICP) using SF₆/O₂ gas mixtures has been optimized to etch the SiC anisotropically and the underlying silicon isotropically with high selectivity using the patterned SiO₂ etch mask.

The fabricated cantilever and bridge structures have been tested dynamically by attaching them to a piezoelectric disk with a low-melting-point soft wax and vibrating them in a vacuum system. The piezoelectric disk has been driven from a swept sine source and the vibration of the beams as a function of frequency has been detected using an optical vibrometer, the experimental set-up of which has been detailed elsewhere.^{6,7} To gain more understanding of the effect of stress in our resonators, simulation of the fabricated structures has been performed using finite element technique (ANSYS) whereby the theoretically predicted resonant frequencies of the devices have been compared with the measured resonant frequencies.

III. RESULTS AND DISCUSSION

The process flow in Fig. 1 shows that using the SiO₂ layer as an etch mask, the optimized SF₆/O₂ plasma first etches the SiC layer anisotropically because of the dominance of the ion-induced etch mechanism⁸ and then continues to etch the Si substrate underneath isotropically with a high selectivity to the SiO₂ mask due to the spontaneous reaction between the F atoms in the SF₆ and Si substrate. The undercut step finally releases the cantilevers and bridges and forms suspended structures. It has been reported that 20% O₂ in the gas mixtures is an optimum condition corresponding to higher etch rates.⁹ In this work, the optimized etching condition chosen for the fabrication of the SiC beams as well as their release has been 40 sccm SF₆ and 10 sccm O₂, 5 mT work pressure, 1000 W ICP coil power, and 50 W chuck power corresponding to about −96 V dc bias. Under these conditions, a SiC etch rate of 276 nm/min and silicon etch

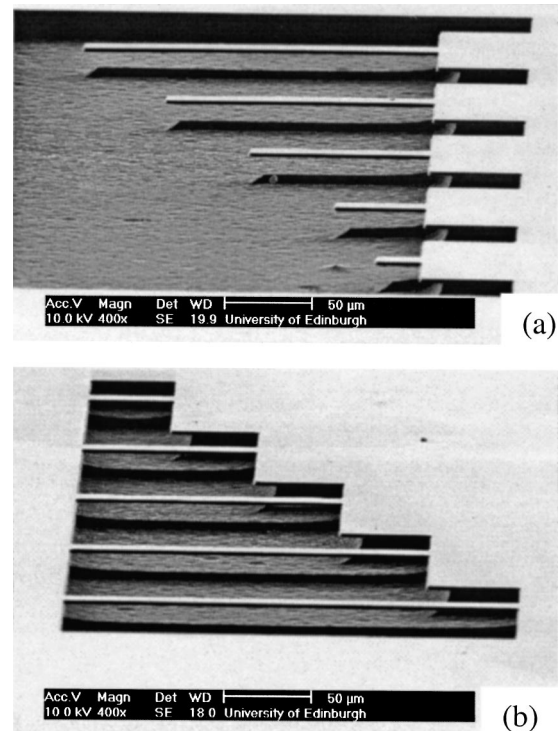


FIG. 2. SEM images of a group of free standing (a) cantilever beams with lengths of 25, 50, 100, 150, 200 μm , respectively and (b) bridges with lengths of 50, 100, 150, 200, 250 μm , respectively. All the beams are 15 μm wide and nominally 2 μm thick.

rate of 2.7 $\mu\text{m}/\text{min}$ have been found. A single-crystal reactive etching and metallization (SCREAM) process has been reported previously¹⁰ to fabricate Si MEMS structures using the thermal oxide layer to protect the sidewalls of the top structures and therefore create great etch selectivity between top structure layer and the substrate layer during the release process. In our experiment, the etch selectivity of about 10:1 for Si to SiC means that SiC can automatically act as an outstanding mask material during the Si substrate etching, thus releasing the resonance devices.

After the release etch, the longest cantilever structure has been observed to be slightly bent downwards, probably due to the stress induced by the SiO₂ onto the SiC. After removal of the remaining SiO₂ layer in hydrofluoric acid and rinsing the samples in deionized water, straight cantilever and bridge structures have been achieved as shown in Figs. 2(a) and 2(b). This postrelease wet etch procedure did not result in obvious damage to the beam structures. Figures 3(a) and 3(b) show close-up scanning electron microscopy (SEM) images of a 25 μm long cantilever and a 50 μm long bridge where the anisotropic etching of the SiC beam and isotropic Si etching underneath the SiC layer can be clearly observed. The straightness of cantilever beams in the absence of the SiO₂ mask indicates the absence of stress gradient within the SiC film.

The cantilevers and bridges have been mechanically actuated and the fundamental resonant frequencies have been measured in a vacuum system. In addition, the fabricated structures have been simulated (including the existence of

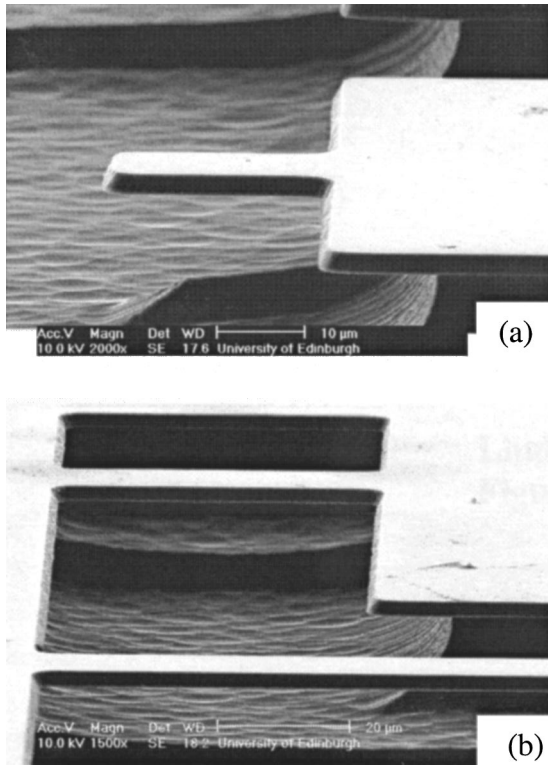


FIG. 3. SEM images of (a) a 25 μm long cantilever and (b) a 50 μm long bridge.

undercut) in order to compare the theoretically predicted resonant frequencies to the measured resonant frequencies. SiC thickness of 2 μm was initially used during the simulation for both cantilevers and bridges. Figures 4(a) and 4(b) show fundamental resonance peaks of 200 μm long cantilever and bridge, respectively. The experimentally measured and the theoretically simulated resonant frequencies of all the fabricated beams are listed in Tables I(a) and I(b). A correction factor has been used to quantify the discrepancy between the theoretically predicted and the experimentally measured fundamental resonant frequencies. The correction factor is calculated from the measured frequencies divided by the correspondingly simulated frequencies. It is evident that the correction factors for the cantilevers are almost constant while the correction factors for the bridges decrease with decreasing bridge lengths. For the cantilevers, it is possible to match the simulated resonant frequencies to the measured frequencies by taking into account the possible variation in the SiC layer thickness. SEM measurement has shown SiC thickness of about 2.9 μm. Therefore, in this case, using a SiC layer thickness of 3 μm instead of 2 μm would bring the theoretical and measured values into alignment, i.e., a correction factor of 1.

The correction factors for the bridges in Table I are not constant which indicates that the discrepancy between the measured and simulated frequencies is not only due to thickness variations for the bridge structures. The higher measured frequencies could result from the existence of stress in the bridge structures. The equation relating the natural fre-

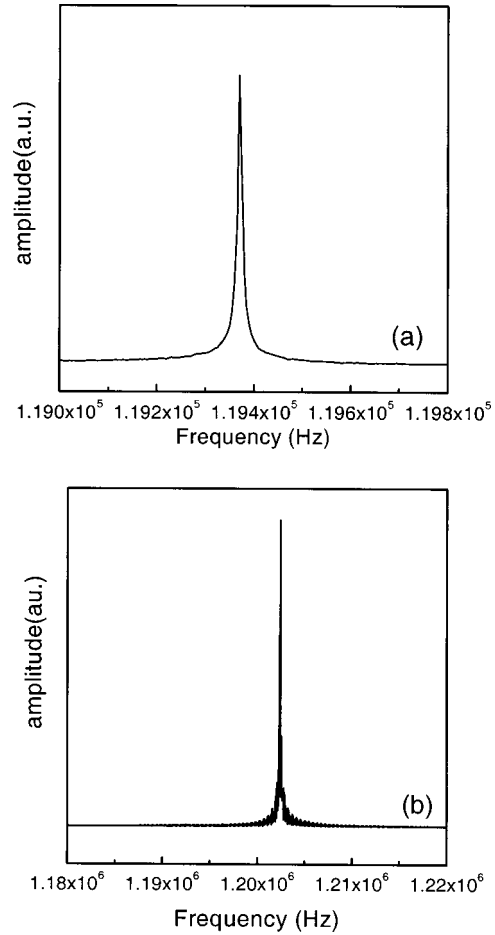


FIG. 4. Fundamental resonance peak of 200 μm long (a) cantilever (b) bridge structures.

quency of a bridge to the degree of stress along its length is as follows:

$$\omega^2 L^4 = \alpha + \beta PL^2,$$

where ω is 2π times the frequency of the stressed bridge, α and β are constants depending on beam material and dimen-

TABLE I. Measured and simulated fundamental resonant frequencies of (a) cantilevers (b) bridges of different length.

	Cantilever length	Measured frequency	Simulated frequency	Correction factor
(a)	200 μm	119.4 kHz	81.5 kHz	1.47
	150 μm	208.6 kHz	142.9 kHz	1.46
	100 μm	451.7 kHz	305.9 kHz	1.48
	50 μm	1.59 MHz	1.08 MHz	1.47
	25 μm	5.05 MHz	3.37 MHz	1.5
	Bridge length	Measured frequency	Simulated frequency	Correction factor
(b)	250 μm	898 kHz	322.2 kHz	2.79
	200 μm	1.2 MHz	491.5 kHz	2.44
	150 μm	1.79 MHz	838.6 kHz	2.13
	100 μm	3.3 MHz	1.73 MHz	1.91
	50 μm	Out of range	5.33 MHz	*

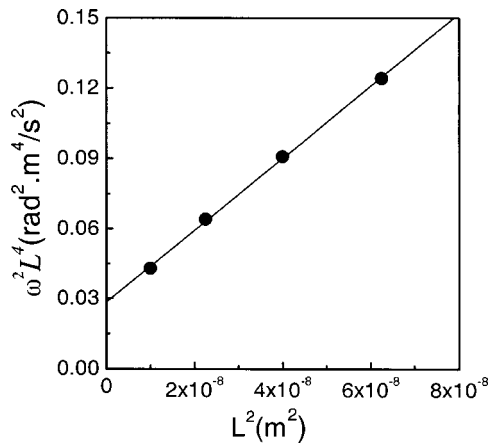


FIG. 5. $\omega^2 L^4$ as a function of L^2 for bridge structures showing linear fit.

sions, L is the length of the beam and P is the stress in the bridge. Figure 5 shows a plot of $\omega^2 L^4$ as a function of L^2 which follows a linear trend. This result shows that the bridges are under tensile stress and the constant slope of the fitted line indicates that the degree of tension is independent of the bridge length. Assuming stress-free and string-mode shapes for the bridges, a significant tensile stress of about 400~500 MPa can be estimated. The intercept of the fitted line corresponds to the value of $\omega^2 L^4$ for bridge structures in the absence of stress, from which the unstressed frequency of a bridge of length L can be determined.

IV. CONCLUSIONS

A one-step dry etching method has been developed to fabricate suspended SiC cantilever and doubly clamped bridge structures using SF₆/O₂ ICP plasma. The dry etch condition has been optimized to take advantage of the anisotropic etch of the SiC layer and the isotropic Si etch (for the release) as well as the high selectivity between the SiO₂

mask and the Si layer. Straight cantilever and bridge structures have been fabricated successfully and the resonant frequencies of the devices have been theoretical simulated and experimentally measured. By comparing the theoretically simulated and experimentally measured resonant frequencies, it has been found that the cantilever beams are free of stress while the bridge structures are under significant tensile stress whose magnitude is independent of the bridge length. Our results show that when designing bridge structures employing cubic SiC grown on silicon, the possible existence of stress should be taken into account.

ACKNOWLEDGMENTS

This work was supported by Engineering and Physical Sciences Research Council (EPSRC) Grant No. GR/R38019/01.

- ¹M. Mehregany, C. A. Zorman, N. Rajan, and C. H. Wu, Proc. IEEE **86**, 1594 (1998).
- ²Y. T. Yang, K. L. Ekinci, X. M. H. Huang, L. M. Schiavone, M. L. Roukes, C. A. Zorman, and M. Mehregany, Appl. Phys. Lett. **78**, 162 (2001).
- ³A. A. Yasseen, C. A. Zorman, and M. Mehregany, J. Microelectromech. Syst. **8**, 237 (1999).
- ⁴A. A. Yaseen, C. H. Wu, and M. Mehregany, in Technical Digest 12th Annual International Conference on MEMS, 17–21 January 1999, edited by K. Gabriel and K. Najafi (unpublished).
- ⁵C. A. Zorman, A. J. Fleischman, A. S. Dewa, M. Mehregany, C. Jacob, and P. Pironz, J. Appl. Phys. **78**, 5136 (1995).
- ⁶J. Hedley, A. J. Harris, J. S. Burdess, and M. E. McNie, SPIE Proceedings on Design Test, and Packaging of MEMS/MOEMS, 2001, Vol. 4408, p. 402 (unpublished).
- ⁷J. S. Burdess, A. J. Harris, D. Wood, R. J. Pitcher, and D. Glennie, J. Microelectromech. Syst. **6**, 322 (1997).
- ⁸N. O. V. Plank, M. A. Blauw, E. W. J. M. van der Drift, and R. Cheung, J. Phys. D **36**, 482 (2003).
- ⁹Liudi Jiang, R. Cheung, R. Brown, and A. Mount, J. Appl. Phys. **93**, 1376 (2003).
- ¹⁰Kevin A. Shaw, Z. Lisa Zhang, and Noel C. MacDonald, Sens. Actuators A **40**, 63 (1994).